Construction and Reactivity Screening of a Surface Composition Gradient for Combinatorial Discovery of Electro-Oxidation Catalysts

Shrisudersan Jayaraman and Andrew C. Hillier*

Department of Chemical Engineering, Department of Chemistry and Institute for Combinatorial Discovery, Iowa State University, Ames, Iowa 50011-2230

Received July 16, 2003

Materials possessing gradients in composition or structure are of interest for a range of applications, including the construction of functionally graded structural materials,[1,2] as novel sensor and actuator platforms,[3] and to control the site-specific binding of proteins and cells on surfaces.[4] Gradients can also be used as sample libraries for combinatorial materials discovery that present an extremely dense sample set.[5]

Combinatorial libraries are frequently constructed through sequential "split and pool" or "split and mix" processing steps that generate large but discrete sample libraries.[6] Ultimately, these library formats represent incomplete data sets that miss potentially active materials existing between the discretely prepared zones. Here, we show a novel gradient fabrication technique for the construction of highly dense sample libraries that exploits solution diffusion followed by electrodeposition to construct a surface gradient. We illustrate the capability of this method for combinatorial discovery of heterogeneous catalysts by interrogating a platinum−ruthenium composition gradient for its activity toward hydrogen oxidation with a reactivity-mapping technique based upon the scanning electrochemical microscope.

The discovery of improved catalysts for low-temperature fuel cells is a particularly promising application of combinatorial materials discovery.[7] In fuel cells, carbon monoxide (CO) poisoning represents a major problem because CO is often present in the anode feed as a result of upstream reforming or is produced as an intermediate during the direct oxidation of liquid fuels.[8,9] During hydrocarbon reforming, the amount of CO produced can exceed 100 ppm, which is well above the acceptable tolerance limit for single-phase Pt catalysts.[9] The addition of oxophilic elements, such as ruthenium (Ru), molybdenum (Mo), osmium (Os), and tin (Sn), to platinum can improve poison tolerance.[9] These additives typically form surface oxides more readily than Pt and, therefore, oxidize CO from the catalyst surface at lower potentials to liberate catalytically active sites.[10] Given the large number of candidate metals and the vast composition space that must be sampled to thoroughly investigate the potential binary, ternary, and quaternary catalyst candidates, combinatorial methods may prove the only practical discovery method.

Scheme 1. Schematic of Gradient Fabrication by Gel-Transfer Deposition

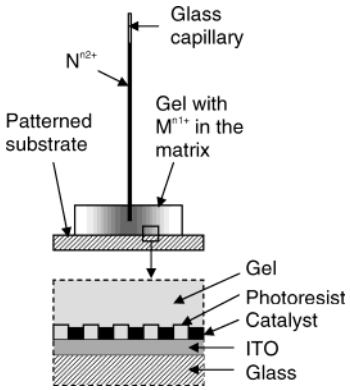

Although array-based samples are the most commonly used library platform in combinatorial catalysis studies, gradients are particularly appealing in that a complete and highly dense composition spread can be constructed. A variety of methods for the construction of gradients have been reported, including liquid and gas diffusion,[4,11,12] diffusion in microfluidic networks,[13] STM-based replacement lithography,[14] physical vapor deposition at oblique angles of incidence,[4,15] and imposed electrochemical[16,17] or electric fields.[18,19] Gradients have been used for numerous applications, including the study of protein interactions with surfaces,[12] induced motion of liquid drops,[11] demixing in lipid bilayer membranes,[19] substrate-induced liquid crystal orientation,[15] imaging the spatially controlled oxidation of hydrogen peroxide,[16] and studies on spatially localized metal deposition.[16,17] Recently, combinatorial studies have demonstrated the use of gradient libraries to examine temperature- and thickness-dependent polymer thin-film dewetting,[20] construct phase diagrams,[21] study mushroom-to-brush crossover in surface anchored polyacrylamide films,[22] and perform coverage-dependent reactivity mapping of heterogeneous catalysts.[17]

In the fabrication method described here, a surface gradient is created by controlled diffusion of precursor materials into a swollen polymer gel.[23,24] Specifically, a binary composition gradient is produced by diffusion of a solution containing the salt of a second metal (N^{n2+}) into a gel containing a uniform concentration of a salt of the first metal (M^{n1+}) in its matrix (Scheme 1). Diffusion is carried out in a controlled humidity enclosure to prevent shrinkage of the gel. Following diffusion, the metal ions are electrochemically reduced onto the surface of a conductive substrate while the substrate is immersed in a conductive electrolyte. Removal of the gel leaves a composition gradient of the binary catalyst system M_xN_y on the substrate.

A binary Pt_xRu_y composition gradient was constructed as a model system. An optical image of a typical gel construction depicts an aqueous solution of $RuCl_3$ diffusing into a 3% agarose gel that was previously loaded with H_2PtCl_6 (Figure 1). The $RuCl_3$ solution is injected from a small glass

* To whom correspondence should be addressed. E-mail: hillier@iastate.edu.

10.1021/cc034030k CCC: $27.50
Published on Web 11/20/2003

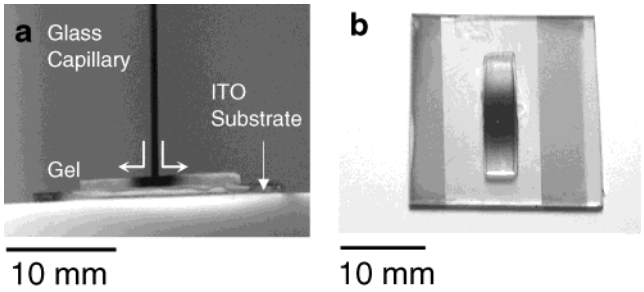

Figure 1. Optical images of gel-transfer deposition. (a) Image showing a layer of swollen gel containing a precursor of the first metal ion ($M^{n1+} = Pt^{4+}$) with a glass capillary piercing the center of the gel to provide a source for diffusion of the second metal ion ($N^{n2+} = Ru^{3+}$). (b) Top view of fully developed Ru^{3+} gradient (black) in Pt^{4+} containing gel (clear). The metal ions are subsequently deposited on the substrate by electrochemical reduction from the gel.

capillary positioned at the center of a rectangular section of gel. Diffusion is allowed to proceed for a period sufficient to establish a spread of Ru^{3+} within the gel. Following removal of the capillary tube, the gel assembly is immersed in a standard three-electrode electrochemical cell, and the gradient in Ru^{3+} and Pt^{4+} precursor salts in the gel are electrochemically reduced to metal on the electrode surface. The gel is subsequently removed to leave the metal deposit on the substrate.[25] Notably, this fabrication method can be performed with any combination of precursor metal salts as long as they are electrochemically reducible and soluble in the gel.

Figure 2a shows a Pt_xRu_y gradient formed on an indium−tin oxide (ITO) substrate using this gel-transfer deposition technique. Scanning electron micrographs (Figure 2b and 2c) of a representative region on the surface illustrate the higher resolution sample structure. A banded pattern can be seen at these magnifications, which arises from a predeposited photoresist mask. The ITO substrate was photolithographically patterned to expose a series of conducting ITO regions separated by insulating photoresist.[26] The photoresist was subsequently removed to provide isolated zones of catalyst along the composition gradient, which was necessary in order to prevent any cross-communication via surface diffusion between various catalyst domains. Atomic force microscopy reveals a reasonably uniform particle size distribution with an average diameter of ∼30 nm (Figure 2d). The composition spread of the Pt_xRu_y sample varied from pure Pt at the edges to almost pure Ru at the center (vide infra). Although it has not been verified that these samples represent true metal alloys, similarly co-electrodeposited catalysts have been reported in alloy form.[27]

Measurement of the activity of the Pt_xRu_y sample toward the hydrogen oxidation reaction was performed using the scanning electrochemical microscope (SECM).[28] The SECM consists of a three-dimensional positioning system that scans an ultramicroelectrode (UME) tip across a substrate at fixed separations while measuring electrochemical current at tip and substrate. Variations in the tip current provide information about reactions occurring at the tip and substrate as well as information about the solution in the tip−substrate gap. SECM has become a routine analytical technique that can perform a range of analyses, including topographic imaging

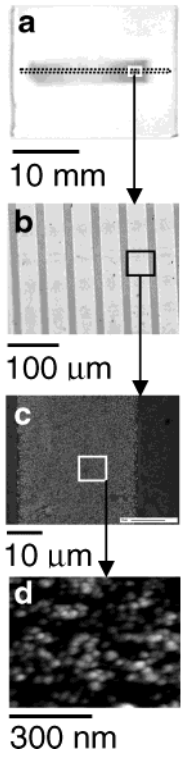

Figure 2. Images of Pt_xRu_y composition gradient. (a) Optical micrograph of the Pt_xRu_y surface gradient. The dashed box reflects the substrate region where subsequent measurements were performed. (b,c) Scanning electron micrographs of the sample at two magnifications showing the banded structure of the catalyst sample. The white regions correspond to that of catalyst deposit, and the darker regions correspond to the bare ITO substrate. (d) Atomic force microscope image of the catalyst particles.

Scheme 2. Schematic of Tip−Sample Interface during Scanning Electrochemical Rate Constant Mapping

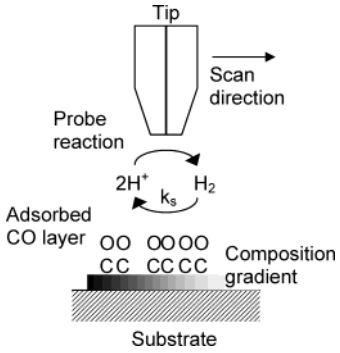

of conductors and insulators; imaging of composition and reactivity in biological systems, including cells and enzymatic reactions; measure kinetics; and detect transport through membranes.[29] In this work, the SECM is used to locally probe catalytic activity. The ability to spatially control the probe tip over a catalyst surface makes it an excellent tool for screening measurements in combinatorial discovery of heterogeneous catalysts.[17,30]

These SECM measurements utilized a 12.5-μm-radius gold tip held at a potential where protons (H^+) in solution are reduced to hydrogen at a diffusion-limited rate (Scheme 2).

$$2H^+ + 2e^- \rightarrow H_2 \qquad (1)$$

At small tip−substrate separations, the tip-produced hydro-

gen can diffuse to the substrate and be oxidized back to protons.

$$H_2 \xrightarrow{k_s} 2H^+ + 2e^- \quad (2)$$

The increase in proton concentration near a reactive substrate generates an increased tip current that is proportional to the hydrogen oxidation rate at the substrate. Knowledge of the tip−substrate separation, tip size, and the tip current allows one to deduce the rate constant (k_s) for the surface reaction by fitting the data to a well-established theoretical model.[29] Notably, the accuracy of the measured rate constant is independent of tip size.[31] However, smaller tip sizes provide a higher spatial resolution and tend to allow a closer approach to the surface, which increases the range of measurable rate constants.

Scanning the SECM tip in close proximity to a substrate surface using the H^+/H_2 probe as the tip reaction provides information about the local catalytic activity of the substrate for the hydrogen oxidation reaction. This is particularly useful for monitoring the kinetics of hydrogen oxidation on a poisoned surface, such as one coated with carbon monoxide. Under these conditions, the tip response is dominated by feedback current due to the hydrogen oxidation reaction. Although the protons generated during CO oxidation could influence the tip response, the presence of only a monolayer of CO on the substrate makes this contribution to the tip current negligible. The spatial resolution of this technique is also particularly appealing for combinatorial studies. On a gradient sample such as the one described here, the SECM reactivity mapping provides a potential spatial resolution that can discriminate between domains on the order of the tip size.[32] Thus, for a 1-in. sample and a 25-μm-diam tip, a single line scan can potentially distinguish between 1200 different catalyst compositions. This information density can be further increased by using smaller tips and scanning over a two-dimensional sample.

In this work, reactivity mapping was combined with surface compositional analysis to deduce the composition dependence of catalytic activity. The composition of the Pt_xRu_y gradient, as determined using energy-dispersive X-ray spectroscopy (EDS), is depicted in Figure 3a. The sample possesses a continuous variation in Ru content down the length of the gradient. The composition profile exhibits a Gaussian shape, which is consistent with axial diffusion of solute from a point source in a semi-infinite slab of gel.[33,34] The highest Ru composition achieved in this sample is 95% at the center (∼11 mm), while pure Pt appears at the edges (2 and 19 mm). Several additional samples were prepared in which the salt concentrations, gel composition and diffusion times were varied in order to modify the size and extent of the composition profile. The exposed composition range could be readily varied by changing these processing parameters.

A reactivity map was constructed to elucidate the effect of CO poisoning on hydrogen oxidation kinetics as a function of Ru composition and electrode potential. This was achieved by performing SECM scans over the gradient sample at several different substrate potentials while holding the tip−substrate separation at a constant value.[35] Figure 3b shows a typical reactivity map for the Pt_xRu_y sample in the presence of adsorbed CO.[36] The image intensity is proportional to the hydrogen oxidation rate, whereas the position reflects the composition and applied potential.

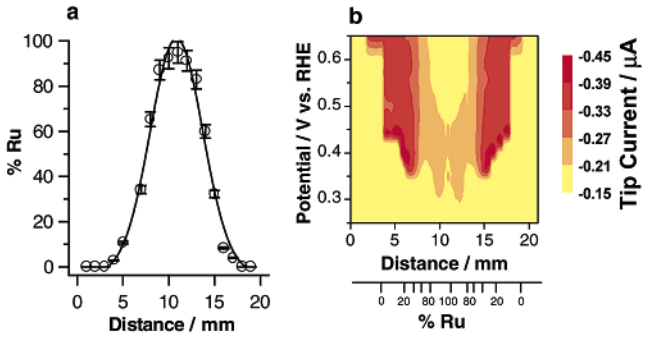

Figure 3. Composition and reactivity maps of Pt_xRu_y gradient. (a) Composition map as a function of distance along the surface as determined by X-ray energy dispersive spectroscopy (EDS). (b) SECM reactivity map of the CO-coated Pt_xRu_y gradient at a tip−substrate separation of 10 μm in a nitrogen-purged aqueous solution containing 0.01 M H_2SO_4 and 0.1 M Na_2SO_4. This image was constructed by combining SECM line scan data acquired at several different substrate potentials.

At potentials below 0.30 V, the tip current is uniform and small, indicating a low hydrogen oxidation rate. Under these conditions, the entire Pt_xRu_y surface is covered with CO, which blocks surface sites required for hydrogen oxidation. Increasing the substrate potential above 0.3 V results in an increase in tip current at select regions of the surface. Increased activity over the background value is first observed at locations of 10 and 12 mm, which represent ∼80% Ru. However, this composition has a very low intrinsic hydrogen oxidation rate as a result of the high Ru content. As the potential is increased to more positive values, additional active zones appear. In particular, two high current zones emerge at positions of 7 and 15 mm at a potential of 0.35 V. These positions reflect the most active catalyst compositions (vide infra). At increasingly positive potentials, the active zones increase in size, which reflects the onset of activity at additional composition values along the gradient. The image appears symmetric about the center, because the Pt_xRu_y composition profile is replicated between the left and right sides of the sample.

At sufficiently positive electrode potentials, CO is completely oxidized, and the entire gradient surface is free of adsorbed CO. This is illustrated by the response at 0.65 V. At this potential, the tip current reflects the intrinsic hydrogen oxidation activity of the surface in the absence of adsorbed CO. At this potential, the ITO region, which does not catalyze the hydrogen oxidation reaction, exhibits a small tip current at positions <2 and >19 mm. A variation in hydrogen oxidation rate can be observed at locations between 2 and 19 mm. The Pt-rich regions exhibit a high tip current, indicating a high activity toward hydrogen oxidation. The tip current decreases with increasing Ru and reaches a minimum at ∼11 mm, which corresponds to the region with maximum Ru content. These observations are consistent with the high activity of Pt and the low activity of Ru for hydrogen oxidation.[10,28] In addition, the formation of ruthenium oxides

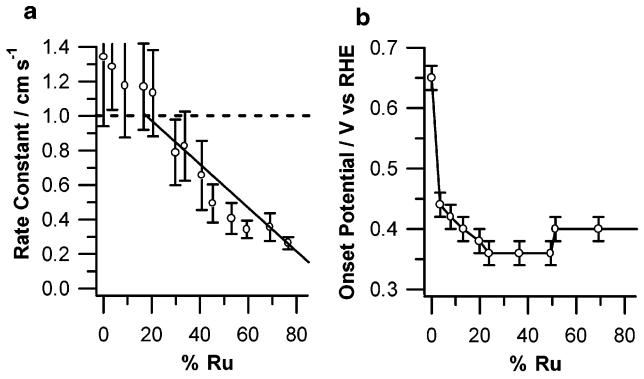

Figure 4. (a) Rate constants for hydrogen oxidation as a function of ruthenium composition for the Pt_xRu_y gradient sample. The figure was constructed by determining values of the rate constants by fitting a theoretical model at several points along a line scan acquired over the Pt_xRu_y gradient in the absence of CO. These data were combined with the composition data in Figure 3a. The dashed line is the diffusion-limited rate constant reflecting the maximum detectable value of k_s with the SECM employed here. The solid line is a linear fit to the data as a guide to the eye showing the decrease in the rate constant with increasing ruthenium content. (b) Onset potential as a function of ruthenium composition. The onset potential was defined as the potential at which the tip current is at least 50% of the value in the absence of adsorbed CO on the catalyst at a given tip−substrate separation.

is illustrated by the decrease in activity with increasing potential for the high Ru content regions near the image center.

The turn-on of activity observed in Figure 3b coincides with the onset of CO oxidation, which frees surface sites for hydrogen oxidation.[37] The origin of this activity is related to the ability of Ru to dissociate water to form surface oxides at low potentials.

$$Ru + H_2O \rightarrow Ru - OH + H^+ + e^- \qquad (3)$$

Subsequent oxidation of surface CO on neighboring Pt and Ru sites is facilitated by adsorbed OH.

$$Ru - OH + CO_{ads} \rightarrow Ru + CO_2 + H^+ + e^- \qquad (4)$$

Once CO is removed from active surface sites, hydrogen oxidation can commence. Relatively few CO-free sites are required to provide substantial hydrogen oxidation rates.[10,38] Therefore, an increase in the hydrogen oxidation rate coincides with the onset of CO oxidation rather than the complete removal of the adsorbed monolayer.

A summary of the reactivity results versus Ru composition is shown in Figure 4. The intrinsic reaction rate for various locations along the gradient is determined by fitting SECM results acquired in the absence of adsorbed CO. Figure 4a depicts the variation of rate constant for hydrogen oxidation as a function of Ru composition for the Pt_xRu_y binary system. At compositions of Ru < 20%, the reactivity is very high. In fact, the measured rate constant for these compositions reaches the diffusion-limited value detectable by SECM in the current configuration, which is in excess of 1 cm s^{-1}.[39] As the Ru content increases above 20%, a near-linear decrease in the reactivity can be observed. The rate constant decreases by more than an order of magnitude at highest Ru content compared to pure Pt. This drop in activity is a consequence of the low intrinsic activity of Ru sites for hydrogen oxidation.

The influence of adsorbed CO on the catalyst activity is summarized in Figure 4b. In this figure, the potential-dependent line scans in Figure 3b are converted into onset potential values. The onset potential was taken as the electrode potential at which the tip current reached at least 50% of the value in absence of adsorbed CO. This was used to indicate when the surface converted from one deactivated by adsorbed CO to one with sufficient free sites to oxidize hydrogen at near-CO-free conditions. A clear variation in onset potential is noted as a function of Ru content. Notably, a decrease of nearly 0.3 V in onset potential is observed for the best Pt_xRu_y composition, as compared to pure Pt. The composition range of 20% < Ru < 50% exhibits the lowest onset potential.

The optimal fuel cell catalyst in this system is the one that possesses high activity for hydrogen oxidation as well as the ability to remove CO at low potentials. In other words, the catalyst possessing the combination of a high rate constant for hydrogen oxidation and a low onset potential for CO oxidation should be the optimum for this reaction. Thus, the optimal composition range from these results gives Pt_xRu_y catalysts in the range 20% < Ru < 30%. This composition range exhibits superior performance compared to others in this binary composition spread. These results are consistent with prior work involving the sampling of discrete[10] or array-type[28] Pt−Ru catalysts for hydrogen oxidation. Although Figure 4b indicates that CO oxidation commences at the lowest potentials for Ru compositions near 80%, this is a less desirable composition because of the low activity for hydrogen oxidation.

In summary, this report demonstrates a novel method for combinatorial library synthesis based upon a gel-transfer deposition technique. When combined with the reactivity mapping capabilities of the scanning electrochemical microscope, this represents a unique tool for the discovery of fuel cell catalysts and possibly other combinatorial studies. The deposition method provides a simple way to controllably construct high number-density gradient samples. Sample preparation by this method is simple in the manner that it does not involve a large number of physical masking-and-deposition steps or complex mixing and delivery techniques. In addition to combinatorial studies, we anticipate the fabrication and reactivity mapping tools outlined in this study will find application in a variety of fields involving creation and characterization of well-defined and spatially varied heterogeneous surfaces.

Acknowledgment. The authors thank the Office of Naval Research for a Young Investigator Award, the National Science Foundation for a CAREER Award, the Camille and Henry Dreyfus Foundation for a New Faculty Award, and the donors of the Petroleum Research Fund as administered by the American Chemical Society for support of this research.

References and Notes

(1) Rawlings, R. *Mater. World* **1995**, *3*, 474−475.

(2) Marple, B. R.; Boulanger, J. *J. Am. Ceram. Soc.* **1994**, *77*, 2747−2750.
(3) Neubrand, A.; Rodel, J. *Z. Metallkunde* **1997**, *88*, 358−371.
(4) Ruardy, T. G.; Schakenraad, J. M.; vanderMei, H. C.; Busscher, H. J. *Surf. Sci. Rep.* **1997**, *29*, 3−30.
(5) Xiang, X.-D.; Sun, X.; Briceno, G.; Lou, Y.; Wang, K.-A.; Chang, H.; Wallace-Freedman, W. G.; Chen, S.-W.; Schultz, P. G. *Science* **1995**, *268*, 1738−1740.
(6) Taylor, S. J.; Morken, J. P. *Science* **1998**, *280*, 267−270.
(7) Reddington, E.; Sapienza, A.; Gurau, B.; Viswanathan, R.; Sarangapani, S.; Smotkin, E. S.; Mallouk, T. E. *Science* **1998**, *280*, 1735−1737.
(8) Ertl, G.; Neumann, M.; Streit, K. M. *Surf. Sci.* **1977**, *64*, 393−410.
(9) Appleby, A. J.; Foulkes, F. R. *Fuel Cell Handbook*; Van Nostrand Reinhold: New York, 1989.
(10) Gasteiger, H. A.; Markovic, N. M.; Ross, P. N. *J. Phys. Chem.* **1995**, *99*, 8290−8301.
(11) Chaudhury, M. K.; Whitesides, G. M. *Science* **1992**, *256*, 1539−1541.
(12) Elwing, H.; Gölander, C. G. *Adv. Colloid Interface Sci.* **1990**, *32*, 317−339.
(13) Dertinger, S. K. W.; Chiu, D. T.; Jeon, N. L.; Whitesides, G. M. *Anal. Chem.* **2001**, *73*, 1240−1246.
(14) Fuierer, R. R.; Carroll, R. L.; Feldheim, D. L.; Gorman, C. B. *Adv. Mater.* **2002**, *14*, 154.
(15) Tingey, M. L.; Luk, Y. Y.; Abbott, N. L. *Adv. Mater.* **2002**, *14*, 1224.
(16) Balss, K. M.; Coleman, B. D.; Lansford, C. H.; Haasch, R. T.; Bohn, P. W. *J. Phys. Chem. B* **2001**, *105*, 8970−8978.
(17) Jayaraman, S.; Hillier, A. C. *Langmuir* **2001**, *17*, 7857−7864.
(18) Lee, K. Y. C.; Klingler, J. F.; McConnell, H. M. *Science* **1994**, *263*, 655−658.
(19) Groves, J. T.; Boxer, S. G.; McConnell, H. M. *Proc. Natl. Acad. Sci. U.S.A.* **1998**, *95*, 935−938.
(20) Meredith, J. C.; Smith, A. P.; Karim, A.; Amis, E. J. *Macromolecules* **2000**, *33*, 9747−9756.
(21) Meredith, J. C.; Karim, A.; Amis, E. J. *Macromolecules* **2000**, *33*, 5760−5762.
(22) Wu, T.; Efimenko, K.; Genzer, J. *J. Am. Chem. Soc.* **2002**, *124*, 9394−9395.
(23) Liedberg, B.; Tengvall, P. *Langmuir* **1995**, *11*, 3821−3827.
(24) Lestelius, M.; Engquist, I.; Tengvall, P.; Chaudhury, M. K.; Liedberg, B. *Colloids Surf., B* **1999**, *15*, 57−70.
(25) A 3% agarose gel containing 1 mM chloroplatinic acid (H_2PtCl_6) in the matrix was first deposited on an ITO-coated glass substrate ($R_s = 6\ \Omega$, Delta Technologies Limited, Stillwater, MN). A glass capillary (i.d. = 0.84 mm) pierced the center of the gel and was filled with a solution containing 50 mM ruthenium chloride ($RuCl_3$) and 0.1 M sodium sulfate (Na_2SO_4). $RuCl_3$ diffused into the gel, creating a concentration gradient of Ru^{3+}. The time of diffusion was 60 min in this study. The substrate was then immersed in a solution of 0.1 M Na_2SO_4, and a potential pulse program with a square wave with potential limits of 0.5 V and −1.0 V vs RHE and a frequency of 100 Hz was applied for 5 min. This resulted in the reduction of the metal ions on the ITO surface forming a co-deposited PtxRuy catalyst gradient. The agarose gel was removed subsequently by dissolving it in a boiling water bath, leaving behind the metal deposit on the substrate.
(26) The ITO substrate was initially patterned using photolithography to expose a series of bands of ∼30-μm width separated by ∼10-μm-wide photoresist bands. A thin layer of the photoresist (Microposit S1813 photoresist, Shipley, Marlborough, MA) was coated on the ITO substrate by spin-coating at 1000 rpm. The substrate was soft-baked in a convection oven at 100 °C for 30 min. The substrate was then exposed to ultraviolet light for 15 min through a patterned mask (Ronchi slide, Edmund Industrial Optics, Barrington, NJ). The substrate was developed immediately (Microposit MF-319 developer, Shipley, Marlborough, MA) leaving behind the unexposed photoresist with the desired pattern. After creation of Pt_xRu_y gradient, the photoresist was removed by immersing the substrate in photoresist remover (Microposit remover 1165, Shipley, Marlborough, MA) for ∼2 min. The substrate was cleaned thoroughly with deionized water before performing any further experiments.
(27) Cattaneo, C.; de Pinto, M. I. S.; Mishima, H.; de Mishima, B. A. L.; Lescano, D.; Cornaglia, L. *J. Electroanal. Chem.* **1999**, *461*, 32−39.
(28) Jayaraman, S.; Hillier, A. C. *J. Phys. Chem. B* **2003**, *107*, 5221−5230.
(29) Bard, A. J.; Mirkin, M. V. *Scanning Electrochemical Microscopy*, 1st ed.; Marcel Dekker: New York, 2001.
(30) Shah, B. C.; Hillier, A. C. *J. Electrochem. Soc.* **2000**, *147*, 3043−3048.
(31) Bard, A. J.; Mirkin, M. V.; Unwin, P. R.; Wipf, D. O. *J. Phys. Chem.* **1992**, *96*, 1861−1868.
(32) The spatial resolution of the SECM is related to the tip size and the tip−substrate separation. The best point-to-point resolution is on the order of the diameter of the active tip area.
(33) Cussler, E. L. *Diffusion: Mass Transfer in Fluid Systems*, 2nd ed.; Cambridge University Press: New York, 1997.
(34) Diffusion in the gel can be approximated by axial diffusion of solute in a semi-infinite slab and can be described by the following equation and boundary conditions: $(\partial C_{Ru^{3+}}/\partial t) = D_{Ru^{3+}}(\partial^2 C_{Ru^{3+}}/\partial z^2)$. Boundary conditions: (i) $t = 0$, all z, $C_{Ru^{3+}} = 0$; (ii) $t > 0$, $z = 0$, $C_{Ru^{3+}} = C^0_{Ru^{3+}} = 50$ mM; (iii) $t > 0$, $z = \infty$, $C_{Ru^{3+}} = 0$. Here, $C_{Ru^{3+}}$ = concentration (M) of Ru^{3+} in the gel in M, t = time (s), z (cm) is the position along the gel with the center of the gel corresponding to $z = 0$, $D_{Ru^{3+}}$ = diffusion coefficient ($cm^2\ s^{-1}$) of Ru^{3+} in the gel and $C^0_{Ru^{3+}}$ = concentration of Ru^{3+} solution introduced into the gel at $z = 0$. Solving the above system results in the following equation for the concentration of Ru^{3+} at any point, z, inside the gel at a given time, t: $C_{Ru^{3+}} = C^0_{Ru^{3+}} \times \mathrm{erfc}(z/\sqrt{(4D_{Ru^{3+}}t)})$.
(35) The tip was scanned well beyond the catalyst region and onto the bare ITO regions. The ITO regions exhibited a pure negative feedback because they are catalytically inactive toward the hydrogen oxidation reaction. This facilitates identifying the edges of the catalyst region as seen by the UME tip, which in turn provides an absolute indexing of the various catalyst compositions as a function of distance, and hence, a one-to-one correspondence with the composition data measured by EDS.
(36) Carbon monoxide was dosed onto the substrate by holding the substrate potential at 0.05 V vs RHE in a CO-saturated solution of 0.01 M H_2SO_4/0.1 M Na_2SO_4 for ∼10 min. CO was then removed from solution by purging with nitrogen for a period of 15 min with the substrate under potential control.
(37) Watanabe, M.; Motoo, S. *Electroanal. Chem. Interfacial Electrochem.* **1975**, *60*, 275−283.
(38) Jambunathan, K.; Shah, B. C.; Hudson, J. L.; Hillier, A. C. *J. Electroanal. Chem.* **2001**, *500*, 279−289.
(39) For a 12.5-μm-radius gold UME, the maximum detectable rate constant is 1 cm s^{-1}, which corresponds to the diffusion-limited detection limit. This means that the actual rate constants for hydrogen oxidation for samples with Ru < 20% are probably higher, but the values detected by the SECM are limited to <1 cm s^{-1} for the present system.

CC034030K